Acceleration and Spatial Reorganization of Bank Erosion under Prolonged Sediment Starvation: Multi-decadal Evidence from the Vam Nao Channel

Nguyen Dam Quoc Huy[1,2], Le Thi Thuy Van[1,2], Tran Thi Kim[1,2*]

[1]University of Science, 227 Nguyen Van Cu, Cho Quan Ward, Ho Chi Minh City 700000, Vietnam
[2]Vietnam National University, Dong Hoa Ward, Ho Chi Minh City, Vietnam
[*]Corresponding author. Email: ttkim@hcmus.edu.vn (0000-0001-5748-3371)
E-mail: ndqhuy@imhoen.com.vn, lttvan@hcmus.edu.vn, and ttkim@hcmus.edu.vn
Keywords: Vam Nao channel, QSCAT, Remote Sensing, Sediment Starvation

Abstract

The reduction in sediment supply in major deltas worldwide is altering the morphological dynamics of river delta systems. However, the way in which this process leads to the spatial reorganization of erosion has not yet been fully quantified. This study analyzes shoreline variations in the Vam Nao channel, Mekong Delta, over the period 1988–2025 in order to clarify the morphological changes of this key distributary reach under conditions of prolonged sediment deficit.

The results show that sediment load decreased at a rate of approximately −2.62 Mt/year at Tan Chau and −0.99 Mt/year at Vam Nao, reflecting a system-wide sediment deficit. At Vam Nao, erosion area increased markedly during the period 1993–2011, with the emergence of continuously eroding segments and large negative LRR. The concurrent increase in the morphological index asymmetry Index AI (up to 0.72–0.88) and the coefficient of variation CV (up to 0.47) indicates that erosion not only intensified in magnitude but also became asymmetric and shifted toward the right bank of the river. In the period after 2012, although AI index remained at a high level, the decrease in CV suggests that erosion zones had been established and became more spatially stable.

These results indicate that the Vam Nao channel system initially shows that this area has undergone a morphological regime shift, from a relatively balanced state to a highly dynamic state and subsequently to a structurally organized erosional state. This study highlights the importance of analyzing the spatial structure of erosion in identifying early signals of morphological transitions in river systems affected by sediment deficit worldwide.

(1) This is a non-peer reviewed preprint on EarthArXiv, and (2) the manuscript is also under review at Environmental Research Communications.

1. Introduction

The morphological stability of large alluvial river systems depends on a dynamic equilibrium between water discharge and sediment supply (Leopold *et al.* 2020, Paola and Voller 2005). When sediment supply declines over a prolonged period, the river system shifts to a state of sediment starvation, increasing bank erosion, lowering the riverbed, and restructuring channel morphology (Darby *et al.* 2016). In recent decades, sediment starvation has been documented in many large river systems worldwide, where hydropower development and sand mining have disrupted natural sediment transport (Kondolf *et al.* 2014, Kummu *et al.* 2010). However, the way in which sediment deficit leads to spatial morphological regime shifts, although quantified in many studies (Wang *et al.* 2015, Frascati and Lanzoni 2009, Delong *et al.* 2021, Phillips *et al.* 2022), has not yet been fully quantified at the scale of key river reaches. At the Mississippi Delta, Edmonds et al. (2023) demonstrated that anthropogenic interventions (dams, levees, extraction) alter sediment balance, leading to sediment deficit and wetland loss in the Mississippi Delta, which is a long term consequence of altered sediment budgets (Edmonds *et al.* 2023). Murphy et al. (2025) also provided a comprehensive analysis of long term trends in suspended sediment (SS) in the lower Mississippi River and Atchafalaya River by applying the WRTDSplus model. The results show a consistent decline in total SS, fine SS, and coarse SS across all 11 stations in both analysis periods (1992–2021 and 2012–2021). The strong reduction in the fine sediment fraction is the dominant factor controlling the overall trend, while coarse sediment also decreased over a wide area (Murphy *et al.* 2025). Similarly, in the Yangtze River, recent analyses show that the significant reduction in sediment load after the operation of large reservoirs has led to riverbed incision and changes in erosion–deposition morphology in tidal influenced reaches (Ge *et al.* 2025). The study by Ge et al. (2025) indicates that reduced sediment supply not only alters the overall mass balance but also promotes the spatial redistribution of erosion, with a stronger concentration toward deep channels and highly dynamic outer banks. Wang (2025) used trend analysis and mutation detection methods to identify synchronous changes between flow and sediment (Wang 2025). Although this approach provides evidence of changes in the dynamic regime, it has not directly tested whether changes in sediment transport lead to a morphological regime shift expressed through the spatial reorganization of erosion.

At the morphological scale, the study by Wen et al. (2025) on the Yellow River analyzed changes in river cross sectional morphology and their response to variations in the flow–sediment regime in the middle reach of the system (Longmen station) during the period 1974–2021. The results show a clear shift from a deposition dominated state (1974–1987) to a prolonged erosional and bed incision state (2007–2021). In particular, the cross sectional shape changed from a near-rectangular form to a U-shaped form, with a tendency for deeper erosion toward one bank, reflecting the internal adjustment of the channel under conditions of reduced sediment supply (Wen *et al.* 2025). Các Remote sensing analyses and field surveys also show significant morphological adjustments in estuarine and deltaic regions. The study by Ma et al. (2025) quantified changes in erosion–accretion area at the Yellow River mouth during the period 1996–2021. The results show that the estuarine morphology underwent four distinct adjustment phases, reflecting changes in the

water–sediment balance before and after the implementation of the Water and Sediment Regulation Scheme since 2002 (Ma *et al.* 2025). These results reinforce the view that sediment reduction can trigger a large scale morphological restructuring process, altering the previous dynamic equilibrium state of the system.

Studies on the Yangtze River (Ge et al. 2025, Wang 2025), Mississippi (Edmonds et al. 2023, Murphy et al. 2025) and Yellow River (Ma et al. 2025, Wen et al. 2025) show that when sediment supply decreases beyond a certain threshold, the system can shift from a dynamic equilibrium state to a state dominated by incision, bank instability, and flow reorganization. These transitions are often accompanied by an increase in the spatial variance of erosion, the formation of localized instability clusters, and changes in longitudinal correlation structure along the river. However, existing studies mainly focus on aggregate flux trends and have not quantified changes in spatial variance or the clustering structure of erosion along the channel.

Most existing studies approach regime shift along two main directions: (i) analysis of changes in total sediment load or riverbed variation at the basin scale (Hou *et al.* 2024, Zhu *et al.* 2024, Li *et al.* 2025); or (ii) numerical modeling to identify morphodynamic thresholds (Wu *et al.* 2023, Brousse *et al.* 2024, Bozzano *et al.* 2024). Meanwhile, the transformation of the spatial structure of erosion, from a diffuse distribution to clustered concentration, has rarely been directly quantified using long term observational datasets. In particular, key distributary reaches within delta systems, which play a role in regulating the distribution of flow and sediment, have hardly been analyzed from the perspective of morphological regime shift based on remote sensing evidence. Moreover, the question of whether this sediment reduction has triggered an intra-delta regime shift, especially at critical distributary reaches, has not yet been systematically examined. This gap creates an important lack of understanding regarding the mechanism of propagation of morphological instability from the basin scale to the reach scale.

The Mekong Delta is one of the largest and most dynamic delta systems in the tropical region, and at the same time is an area strongly affected by the reduction in sediment load since the early 2000s (Van Binh *et al.* 2020, Allison *et al.* 2017). Recent studies show that sediment supply to the delta has significantly decreased compared to the late twentieth century, leading to riverbed lowering and increased bank erosion (Anthony *et al.* 2015, Van Manh *et al.* 2015). However, most existing studies focus on overall variations at the basin or coastal scale, while the process of morphological restructuring at strategic distributary reaches within the delta has not yet been systematically analyzed over long time series. The Vam Nao River plays an important role in the distributary network of the Mekong system in Vietnam. As the connecting reach between the Tien River and the Hau River, Vam Nao controls the distribution of flow and sediment between the two main branches of the delta (Nga *et al.* 2022, Huy *et al.* 2025). Its curved morphology, large depth, and complex hydrodynamic interactions make this reach particularly sensitive to variations in sediment supply (Nga et al. 2022). The high morphological sensitivity of this reach makes it capable of responding strongly to sediment supply reduction, and therefore it may clearly express regime shift.

This study focuses on integrating long term remote sensing analysis with spatial statistics to provide quantitative evidence of morphological change trends under sediment deficit conditions in the Vam Nao River, a key distributary system of the Mekong Delta. The results not only contribute to the understanding of internal morphodynamic processes

within the Mekong Delta, but also provide evidence of changes in the spatial structure of morphological instability. The novelty of this study lies not only in quantifying erosion–accretion area, but also in analyzing spatial structure and changes in morphological variance over a 35 year dataset (1988–2023), allowing the identification of internal reorganization of the system.

2. Study Area

With a length of approximately 6.5 km, Vam Nao is the shortest river in the river system of the Mekong Delta (Figure 1a, red box). In addition, it is also the only natural connection that performs the function of redistributing discharge between the two main branches, the Tien River and the Hau River (Gierszewski *et al.* 2020). According to observational data, when the Mekong flow enters the Vietnam border, the initial flow partition shows a large difference, with 80.47% flowing into the Tien River and only 19.53% into the Hau River. However, through the water transfer mechanism at Vam Nao (about 29.09%), this proportion is significantly balanced downstream. (Figure 1b–d). Although maintaining a stable state during the period 1988–2010, the flow characteristics in this confluence area have recorded complex variations since 2010 (based on data collected from the Southern Regional Hydro-Meteorological Center at the Vam Nao station).

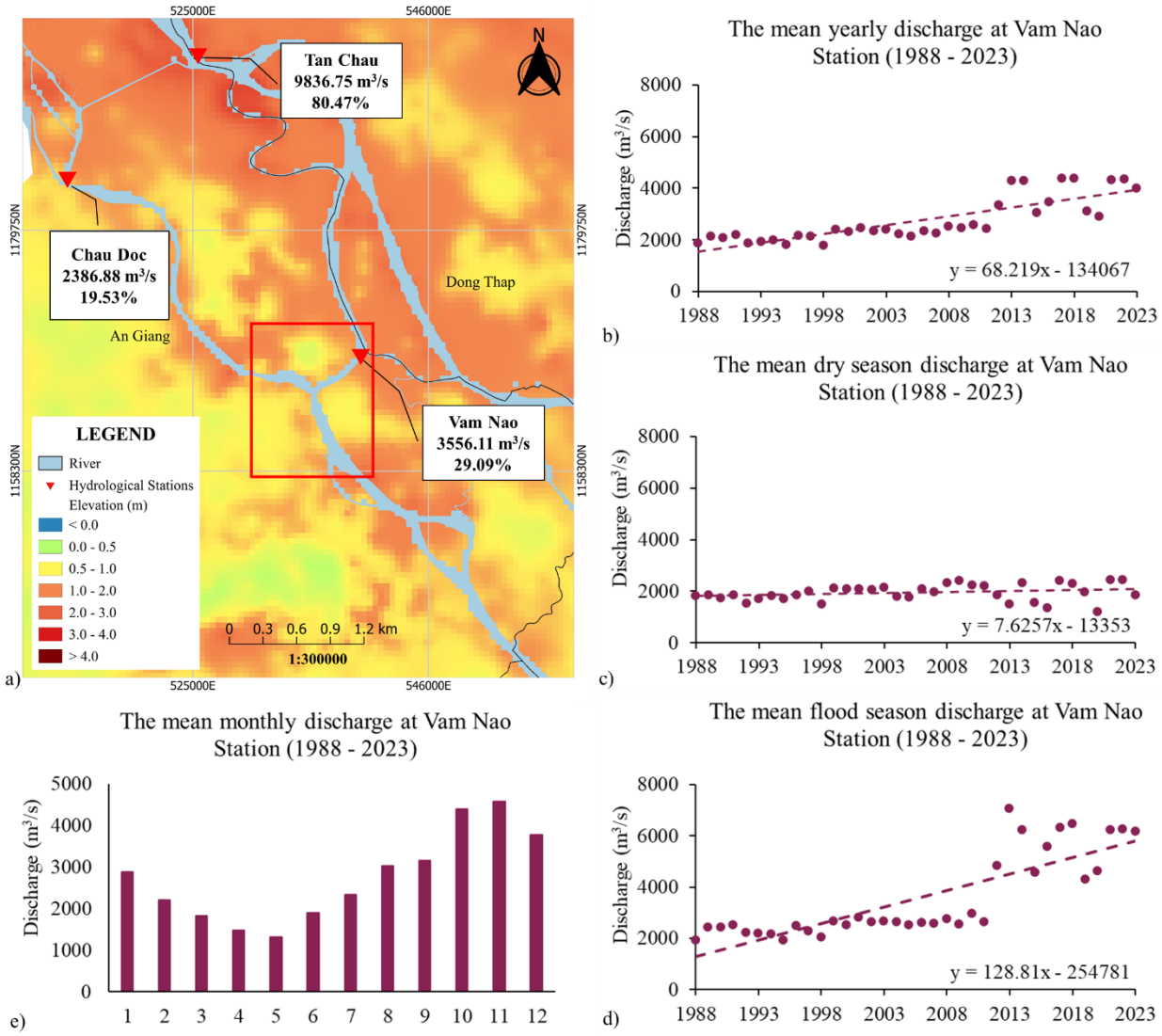

Figure 1. Study area

3. Material and methods

3.1. Data

In this study, all Landsat satellite images, including Landsat 4–5 Thematic Mapper (TM), Landsat 7 Enhanced Thematic Mapper Plus (ETM+), and Landsat 8 Operational Land Imager/Thermal Infrared Sensor (OLI/TIRS), together with Sentinel-2, were collected and used to calculate shoreline variation and its rate of change in the Vam Nao River reach. In addition, suspended sediment data for the period 1985–2023 were also collected from the Southern Regional Hydro-Meteorological Center to clarify one of the factors contributing to the erosion rate.

Table 1. Research data

Data Remote Sensing							
Satellite Image	Number of bands	Spatial Resolution (m)	Revisit Time (Days)	Type of Sensors	Current Status	Green	SWIR 1
Landsat 4-5	7	30 – 120	16	MSS and TM	End on 2013	Band 2	Band 5
Landsat 7	8	15 - 60	16	ETM+	Operational	Band 2	Band 5
Landsat 8-9	11	30 - 100	16	OLI and TIRS	Operational	Band 3	Band 6
Sentinel - 2	13	10 - 60	10 for individual (5 days when combines A and B sensors)	MSI	Operational	Band 3	Band 11

Data Total Suspended Sediment				
Station	Coordinate		Time	Source
	Long	Lat		
Tan Chau	105.25°	10.80°	1985 - 2023	Southern Regional Hydro-Meteorological Center
Vam Nao	105.37°	10.57°	2008 - 2023	

3.2. Research methodology

The research procedure was implemented through an integrated methodological framework consisting of three main stages (Figure 2): Shoreline Change Analysis, Non-Parametric Statistical Testing, and Morphology–Dynamics Correlation Assessment.

First, *Shoreline Change Analysis*: the study collected a time series of satellite images for the period 1988–2025 to be processed on the Google Earth Engine (GEE) platform. The Modified Normalized Difference Water Index (MNDWI) was applied to classify land and water, thereby automatically extracting shorelines based on a thresholding method (Xu 2006). The image processing workflow includes binarization, connected pixel filtering, and vectorization to build an annual shoreline database in GeoJSON format. Next, the QSCAT tool integrated within QGIS software was used to establish transects and calculate statistical indicators of shoreline change (Facun *et al.* 2025). Among these, the Linear Regression Rate (LRR) was primarily used to determine long term trends, combined with NSM, EPR, WLR, as well as asymmetry index (AI) and coefficient of variation (CV) to clarify the regularity of riverbank morphology (Das *et al.* 2013).

Second, *Non-Parametric Statistical Testing*: in parallel with shoreline analysis, total suspended sediment (TSS) data for the period 1985–2023 were compiled and pre-processed using Excel. After estimating annual sediment load, the study used the Python programming language to perform non-parametric tests including Pettitt's test (Pettitt 1979), Mann-Kendall (Kendall 1975) and Sen's Slope (Şen 2012). This stage aims to determine the statistical significance of long term sediment decline trends and to identify change-points in the observed time series.

Finally, *Morphology–Dynamics Correlation Assessment*: the results from the two previous stages were synthesized to conduct a critical analysis of the interaction between morphological changes (shoreline erosion/accretion) and flow dynamics (reduction in sediment supply). Establishing this quantitative relationship allows for a comprehensive assessment of environmental vulnerability and supports the projection of future channel morphology change scenarios in the study area.

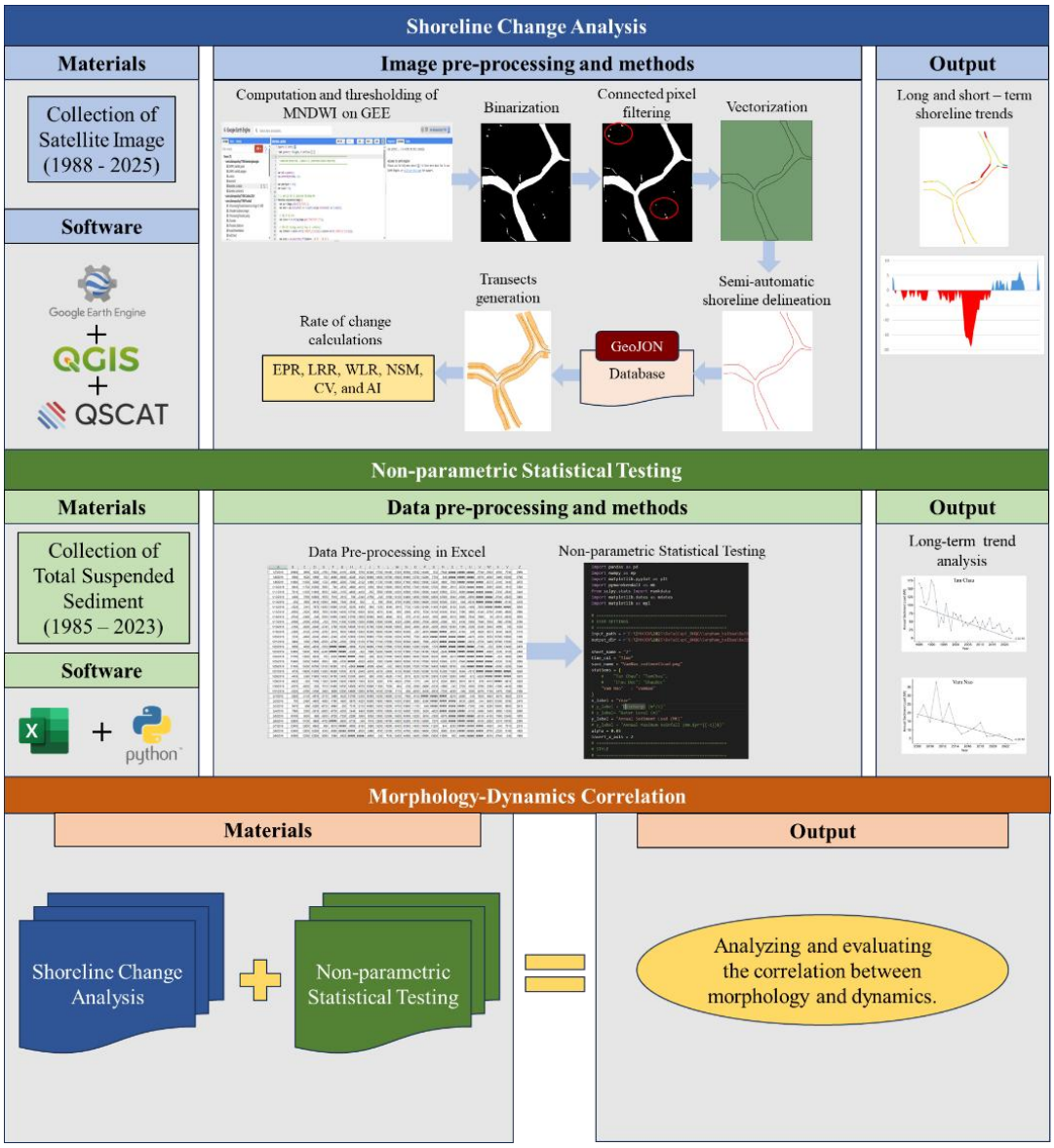

Figure 2. Flow chart of the research.

3.2.1. Non-parametric tests

This study applied non-parametric testing methods to analyze and evaluate the long term TSS data series. First, Pettitt's test was performed to detect statistically significant change points in the data series (Pettitt 1979), then the Mann–Kendall (MK) test was used to identify monotonic increasing or decreasing trends in the time series (Kendall 1975). In parallel, the Sen's slope estimator (Şen 2012) was implemented to quantify the actual magnitude of change, allowing a more accurate determination of the annual sediment load reduction rate with higher reliability compared to conventional linear regression models.

3.2.2. Calculation, thresholding based on MNDWI index and shoreline extraction

The technique using spectral indexs from two is an effective method for extracting water bodies and identifying shorelines from remote sensing images. Several indexs have been used such as NDWI (McFeeters 1996), MNDWI (Xu 2006), AWEI (Feyisa *et al.* 2014) and WI2015 (Fisher *et al.* 2016). However, this study selected MNDWI due to its better and more stable water–land separation capability. According to Xu (Xu 2006), MNDWI outperforms NDWI by reducing noise effects from land surfaces, thereby improving the accuracy of surface water extraction. The MNDWI index is calculated using the following Equation (1):

$$MNDWI = \frac{GREEN - SWIR1}{GREEN + SWIR1} \quad (1)$$

Where: Green is the green band, and SWIR is the Short Wavelength Infrared 1 band. The value of MNDWI ranges from −1 to 1. Table 1 provides detailed information of each image and spectral band used in applying Equation (1).

To classify the land–water boundary, water pixels need to be identified using an appropriate positive threshold (Xu 2018). According to Fisher (Fisher et al. 2016) and Xu (Xu 2018), the optimal threshold is 0 for all land–water classifications. Therefore, this study used a threshold of 0 to automatically delineate the boundary between land and water in the Vam Nao River reach. The entire workflow of MNDWI calculation, thresholding, and shoreline extraction was performed automatically on the Google Earth Engine (GEE) platform (Gorelick *et al.* 2017).

This platform enables remote sensing data processing in a cloud computing environment with direct access to satellite image datasets, performing spectral index calculations, applying classification thresholds, and extracting shorelines consistently for long term time series. Automation on GEE not only reduces errors caused by manual processing but also improves the consistency and reproducibility of the research results.

3.2.3. Methodological uncertainty

The positional error of the shoreline was determined using Equation (2) adopted from the study (Tanwari *et al.* 2025). In addition, the total uncertainty of shoreline positional error ($\mathbf{E_{total}}$), within a specific time period, was calculated using a formula that combines both positional error and measurement error, as presented below:

$$E_{total} = \pm\sqrt{E_{sv}^2 + E_p^2 + E_{gr}^2 + E_d^2} \quad (2)$$

Table 2. Extraction errors from satellite images

Acquisition year	Image type	Shoreline uncertainty (m)					
		Pixel error (E_p)	Seasonal error (E_{sv})	Tidal error (E_t)	Georeferencing (E_{gr})	Digitizing error (E_d)	E_{total}
1988	Landsat 4-5 TM	0	0.61	NA	0	15	15.01
1992	Landsat 4-5 TM	0	0.61	NA	0	15	15.01
1993	Landsat 4-5 TM	0	0.61	NA	0	15	15.01
2011	Landsat 4-5 TM	0	0.61	NA	0	15	15.01
2012	Landsat 8 OLI	0	0.61	NA	0	7.5	7.52
2025	Sentinel - 2	0	0.61	NA	0	5	5.04

3.2.3. Morphological analysis

Asymmetry Index (AI): To assess the degree of asymmetry in erosion between the two banks of the Vam Nao River, this study applied the AI following the method of David Knighton (1981) (Knighton 1981). This index is used to quantify the difference in the intensity of erosion and deposition between the two riverbanks through the relative relationship between morphological variables. The AI is determined using the following equation:

$$AI = \frac{A_R - A_L}{Total} \quad (3)$$

Where: A_R and A_L are respectively the areas of erosion (or deposition) at the right and left banks of the river within the same study period. The AI value ranges from −1 to 1, in which a positive value indicates the dominance of erosion at the right bank, while a negative value indicates that erosion is mainly concentrated at the left bank. An AI value approaching 0 reflects a relative balance between the two banks, indicating a more morphologically stable river system.

Coefficient of variation (CV): The CV is used to quantify the relative variability of shoreline change rates along the study area. CV is defined as the ratio between the standard deviation and the mean shoreline change rate, providing a normalized measure of dispersion. This index allows comparison of shoreline dynamics between different coastal segments regardless of differences in magnitude. A higher CV value indicates greater spatial or temporal variability and less stable shoreline behavior, while a lower value reflects more stable shoreline conditions (Tanwari et al. 2025).

4. Results

4.1. Declining sediment trend

The results of the time series analysis of annual sediment load show a clear and persistent declining trend in the study area, demonstrating high consistency between Tan Chau station and the Vam Nao channel (Figure 3b–c). At Tan Chau station, during the early period (1985–1995), the system was in a sediment-rich state with loads fluctuating

strongly from 100–175 Mt. However, the trend analysis confirmed a continuous decline over more than three decades with a slope (Sen's slope) reaching −2.62 Mt/yr. Statistical testing indicates that this decreasing trend is statistically significant ($p < 0.05$), confirming that this is not a random fluctuation but a systemic change. After 2000, the sediment load dropped sharply to 30–70 Mt and continued to reach extremely low levels (below 30 Mt) after 2015. This statistically significant decline provides evidence of a severe weakening of sediment supply from upstream, placing the river system at risk of serious morphological imbalance.

At the Vam Nao channel, the declining trend was also clearly observed during the period 2008–2023. The annual sediment load ranged from 5–35 Mt, with some local peaks in 2011 and 2013. However, the linear trend shows a decline rate of approximately −0.99 Mt/year, indicating a continuous reduction of sediment transported through this distributary reach. After 2015, the sediment load remained at low levels, mainly below 10 Mt, with smaller fluctuations compared to the previous period, reflecting a more stable but clearly sediment-deficient state.

The analysis results at the two stations show that the declining trend is spatially consistent; however, the magnitude of decline is greater at Tan Chau, reflecting its role as the main source of sediment supply from upstream. The simultaneous decline at both Tan Chau and Vam Nao indicates that sediment deficiency is not only local but systemic, directly affecting the morphological balance in the study area.

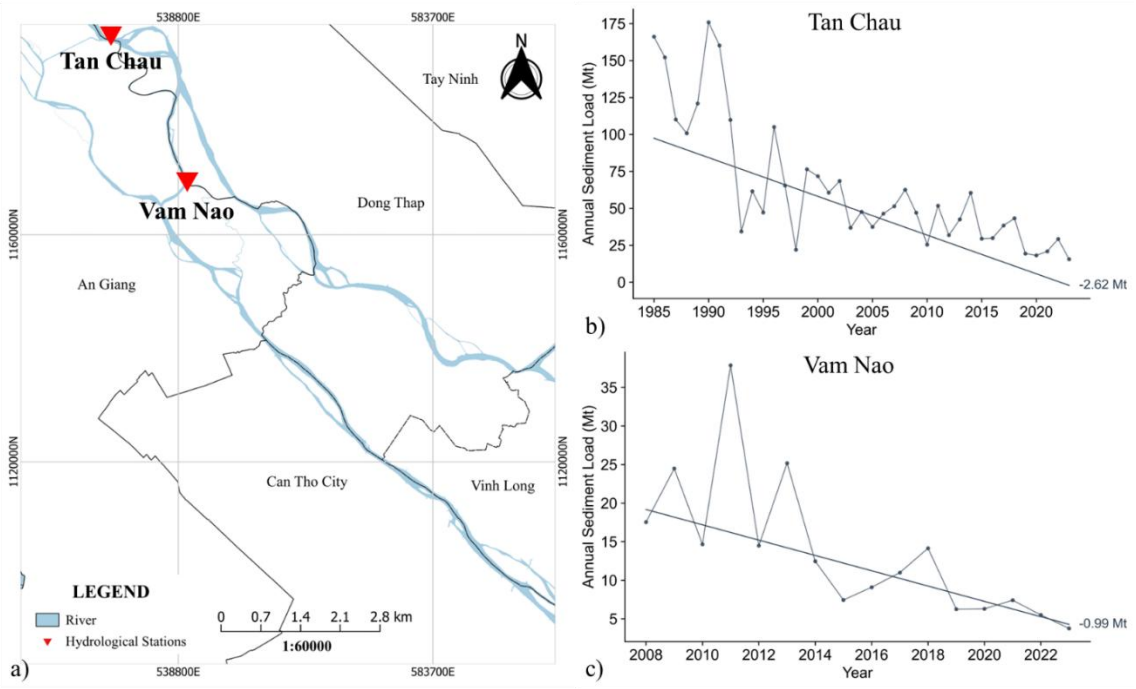

Figure 3. Declining trend of TSS over different periods

4.2. Long term shoreline change (1988–2025)

To comprehensively characterize the morphological response of the Vam Nao channel, three indexes were analyzed, including LRR, AI, and CV. The LRR index represents the intensity of shoreline change, allowing the quantification of the rate and magnitude of

erosion or deposition. The increasingly negative LRR values during the period 1993–2011 indicate a strong increase in bank erosion, reflecting a shift of the system toward an erosion-dominated state. Meanwhile, the AI index reflects the directional nature of morphological processes, indicating whether erosion or deposition tends to concentrate on one bank. The significant increase of AI during the same period (especially in Area1 and Area3) indicates the emergence of clear morphological asymmetry, suggesting that erosion processes are no longer randomly distributed but have become spatially organized. The CV coefficient represents the degree of variability and spatial instability of erosion and deposition processes. High CV values during the transitional period indicate strong spatial heterogeneity, reflecting the formation of erosion "hotspots" and an unstable morphological state.

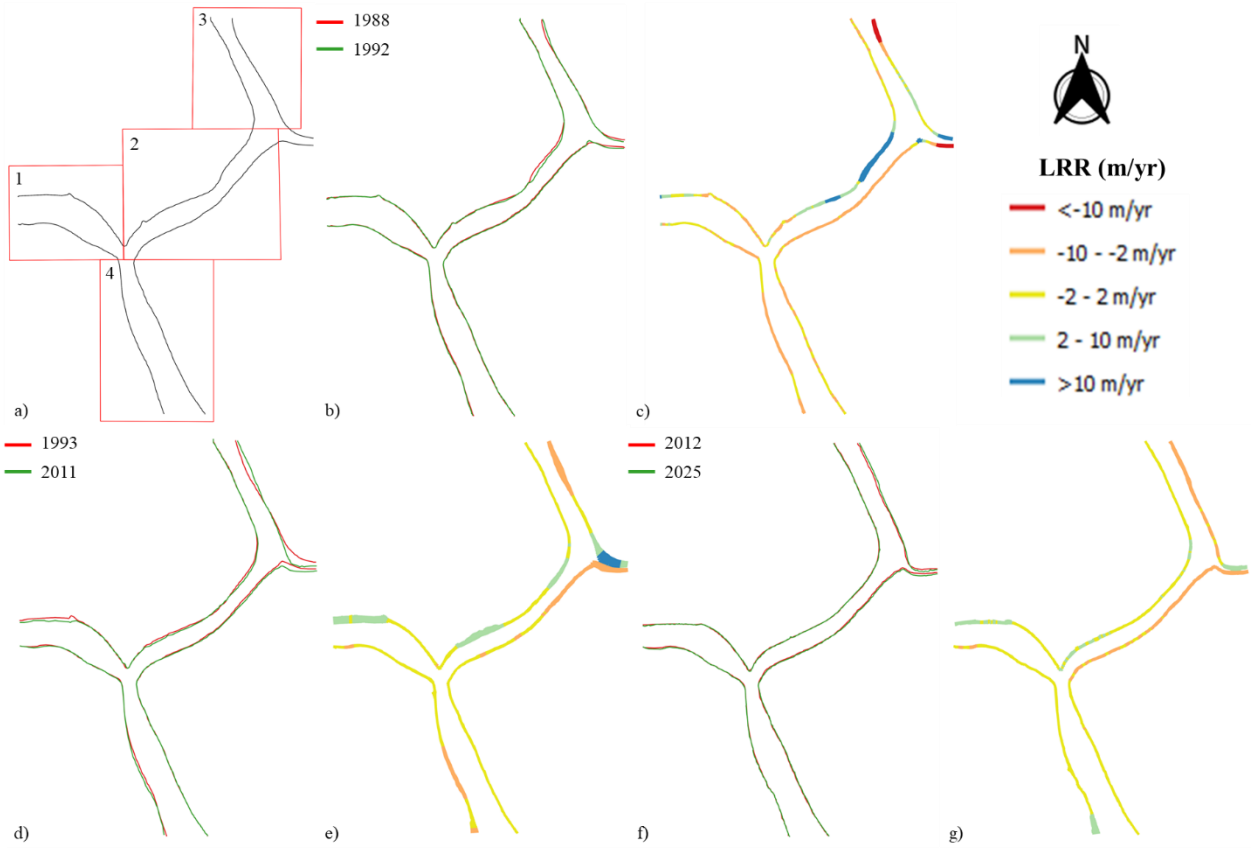

Figure 4. Shoreline evolution over different periods (b, d, f) and shoreline change rate (c, e, g)

Table 3. Statistics of erosion and deposition (unit: ha)

Period	1988-1992			1993-2011			2012-2025		
	Accreting	Eroding	Stable	Accreting	Eroding	Stable	Accreting	Eroding	Stable
Area1	0	6333.12	102899.1	0	258185.3	66551.37	0	32975.67	115781.8
Area2	123595.83	0	78876.91	313506.5	8967.1	45800.31	7077.21	0	30484.89
Area3	25498.13	53967.72	9787.64	88339.51	123024.7	8431.62	58838.58	42944.6	15298.81
Area4	8960.61	38656.62	162306.9	0	438249.5	119397.8	0	171056	132731.8

Across the four study areas, the results indicate an increase in intensity and spatial reorganization of morphological processes over time (Figure 4). Based on the calculated results, three main morphological groups can be identified: (i) erosion-dominated areas (Area1 and Area4), (ii) deposition-dominated area (Area2), and (iii) transitional area (Area3).

The erosion-dominated group (Area1 and Area4) shows a strong increase in erosion intensity during the period 1993–2011. In Area1, the erosion area increased from 6.333 ha (1988–1992) to 258.185 ha (1993–2011), then decreased to 32.976 ha (2012–2025), while the stable area increased from 66.551 ha to 115.782 ha, indicating a decreasing trend in intensity and fragmentation of erosion. In Area4, erosion increased most strongly in the entire system, from 38.657 ha to 438.250 ha, before decreasing to 171.056 ha in the recent period. This increase is associated with large negative LRR values and continuous distribution, reflecting the formation of large scale erosion belts (Figure 4c, e); however, after 2012, the reduction in area and continuity of LRR indicates a process of reorganization and spatial fragmentation of erosion (Figure 4g).

The deposition-dominated group (Area2) maintains a clear deposition trend during most of the study period. The deposition area increased from 123.596 ha (1988–1992) to 313.507 ha (1993–2011), while erosion only appeared at a very small level (8.967 ha). However, during the period 2012–2025, the deposition area sharply decreased to 7.077 ha, and erosion was almost absent, with the stable area at 30.485 ha, indicating a clear weakening of morphological dynamics and a tendency toward a more stable state.

The transitional area (Area3) exhibits the highest and most complex variability, with the coexistence of erosion and deposition in all periods. In the early period, erosion (53.968 ha) exceeded deposition (25.498 ha), indicating an initial imbalance. In the period 1993–2011, both processes increased strongly, with erosion reaching 123.025 ha and deposition 88.340 ha, reflecting a highly dynamic state with large-amplitude and densely distributed LRR values. In the recent period, both erosion (42.945 ha) and deposition (58.839 ha) decreased significantly, indicating that this area is gradually shifting toward a more stable state.

The uneven changes across these areas indicate that the morphological response under sediment-deficient conditions does not occur uniformly, but depends strongly on the local geometric and dynamic conditions of each river reach.

4.3. Morphological change index (AI)

Considering the AI (Table 4) and CV (Table 5) shows a clear increase in the intensity and variability of morphological processes after the period 1992.

During the period 1988–1992, AI in all areas was positive (0.11–0.27), indicating that morphological changes tended to be slightly skewed toward the right bank; however, with low values and CV close to 0, the system still maintained a stable state, with limited variability and relatively uniform distribution.

In the period 1993–2011, AI increased strongly in Area1 (0.72) and especially in Area3 (0.88), indicating high morphological asymmetry, with erosion strongly concentrated on the left bank. Area4 also recorded a significant increase (0.47), while Area2 decreased (0.06), reflecting the stability of morphological variation in this area. At the same time, the CV of both erosion and deposition showed high variability, especially in Area2 (CV erosion: 0.39) and Area3 (CV deposition: 0.47), indicating strong and spatially heterogeneous variability during this period. The simultaneous increase of AI and CV reflects a phase of

morphological imbalance, in which erosion processes not only increased in intensity but also became spatially concentrated in a specific direction.

During the period 2012–2025, AI remained almost unchanged, maintaining high values in Area1 and Area3, indicating that morphological asymmetry was maintained. However, CV decreased clearly in most areas, with many values approaching 0, indicating that the level of variability had reduced. This reflects a transition from a highly dynamic state to a relatively stable structural state, in which zones of change had been established and showed little variation over time.

Table 4. Morphological change index in the four calculated areas

	1988-1992	1993-2011	2012-2025
Area1	0.27	0.72	0.72
Area2	0.11	0.06	0.06
Area3	0.11	0.88	0.88
Area4	0.24	0.47	0.47

Table 5. Variability analysis in the four calculated areas

CV erosion	1988-1992	1993-2011	2012-2025
Area1	0.00	0.08	0.07
Area2	0.00	0.39	0.09
Area3	0.16	0.32	0.16
Area4	0.00	0.15	0.00
CV deposition	1988-1992	1993-2011	2012-2025
Area1	0.00	0.32	0.00
Area2	0.14	0.14	0.00
Area3	0.00	0.47	0.00
Area4	0.00	0.00	0.00

5. Discussion

5.1. Sediment supply change

The analysis results show a clear decline in TSS after 1992, with a reduction of 25–30% at Tan Chau and 40–50% at Chau Doc, reflecting a decrease in sediment supply in the downstream Mekong system. This trend is consistent with previous studies showing that sediment loads to the Mekong Delta have significantly decreased due to the increase of upstream reservoirs and the high sediment trapping efficiency of dam systems (Van Binh et al. 2020, Allison et al. 2017).

The period-based analysis shows that the decline does not occur linearly but follows a stepwise pattern (stepwise decline). The period 1988–1992 is characterized by sediment rich conditions, while the period 1993–2012 shows a moderate declining trend. Notably, after 2010, the system shifted to a clearly sediment deficient state, with TSS values decreasing to low levels and showing less variability. This transition suggests the existence of a structural breakpoint in the sediment supply regime, consistent with Pettitt test results identifying the period 2009–2011 as the main transition point (Huy et al. 2025). The reduction in sediment not only decreases the source of depositional material but also

disrupts the dynamic balance between flow and channel morphology, leading to increased erosion and channel bed lowering, as reported in large systems such as the Mississippi River and the Yangtze River (Edmonds et al. 2023, Ge et al. 2025). In this study, the increase in erosion area and large negative LRR values during the period 1993–2011, especially in Area1 and Area4, indicates a clear morphological response to the decline in sediment supply.

Notably, the AI and CV indexes reach their highest values during the same period, indicating a simultaneous increase in both the intensity and variability of morphological processes. This is consistent with regime shift studies, in which sediment reduction can lead to increased variance and spatial reorganization of erosion (Delong et al. 2021, Phillips et al. 2022). The persistence of high AI but decreasing CV after 2012 suggests that the system may have shifted to a new morphological state with high intensity but lower variability.

5.2. Hydrodynamic forcing

In addition to the decline in sediment supply, flow dynamics play an important role in controlling morphological changes in the Vam Nao channel, particularly through the interaction between the two main flow sources from Tan Chau (Tien River) and Chau Doc (Hau River). Changes in the distribution of discharge between the two river branches play an important role in controlling flow concentration. Hydrological analysis results show that the proportion of flow toward the Hau River decreased from about 42% before 1992 to about 12–17% in recent periods (Huy et al. 2025). This corresponds to the relative discharge in the Tien branch increasing by about 2–3 times compared to the Hau branch during the dry season. This imbalance may lead to an increase in velocity and local shear stress at connecting reaches such as Vam Nao. Therefore, the increase in erosion in areas such as Area1 and Area4 may be related to flow concentration due to discharge redistribution. This indicates that under reduced sediment supply, this imbalance alters the energy distribution in the distributary reach of Vam Nao, leading to the concentration of erosion in specific areas (Nga et al. 2022). Previous studies have shown that in distributary systems, changes in discharge partitioning can lead to morphological reorganization and the formation of concentrated erosion zones (Wang et al. 2015, Li et al. 2025). The period 1993–2011 recorded a strong increase in erosion together with the expansion of reaches with large negative LRR values in Area1 and Area4, indicating the likely presence of flow and energy concentration in these areas.

Curved reaches or those with asymmetric geometry can enhance secondary flow and concentrate erosion toward one side, especially under conditions of imbalance between the two flow sources. The persistence of right-skewed erosion is evidence of the continuous dominance of flow dynamics in this area across all four zones (Blanckaert *et al.* 2010). During the period 2012–2025, although erosion intensity was still maintained in some areas, the decrease in CV indicates that the level of variability has reduced. This suggests a gradual adjustment of the flow system after the channel morphology had significantly changed in the previous period, leading to a redistribution of energy toward a more stable configuration.

5.3. Morphological transition

The analysis results show that the Vam Nao channel system has undergone a clear morphological transition under the combined effects of sediment supply reduction, changes in flow dynamics, and sand mining activities. This process is expressed through three characteristic phases: (i) a relatively balanced state (1988–1992), (ii) a period of strong increase in morphological variability (1993–2011), and (iii) a state of maintaining high variability but with a spatial structure that has been reorganized (2012–2025).

During the initial period, the system maintained a dynamic equilibrium state with high and stable TSS values, low and dispersed LRR, together with low AI and CV values. This reflects a system capable of self-adjustment between sediment transport and flow energy, without the presence of concentrated erosion zones.

After 1992, the clear decline in TSS weakened the supply of depositional material. The period 1993–2012 recorded a strong increase in erosion area, the appearance of reaches with large and continuous negative LRR, together with the simultaneous increase of AI and CV. These characteristics indicate that the system entered a highly dynamic state with a spatially heterogeneous structure, characterized by the formation of concentrated erosion zones.

Notably, in the period 2012–2025, although AI remained high in the main areas, CV decreased significantly and the distribution of LRR became more discontinuous. This indicates that the system did not continue to increase in variability but shifted to a maintenance state, in which erosion zones had been established and showed less variation over time. The combination of high morphological intensity (high AI) and low variability (decreasing CV) is a signal of a restructured morphological state.

Overall, the combination of three main signals including (i) stepwise sediment decline, (ii) the increase and subsequent decrease of morphological variability (CV), and (iii) the formation and fragmentation of erosion zones with large negative LRR, indicates that the system may have undergone a morpho-dynamic regime shift. The results show that the Vam Nao channel system has shifted from a sediment-balanced state to a morphology dominated by erosion, accompanied by spatial reorganization of erosion zones.

5.4. Conceptual framework of morpho-dynamic change under sediment starvation

Based on the integrated analysis of the LRR, AI, and CV indexes, this study proposes a conceptual framework for the morphological transition of river systems under prolonged sediment deficiency. This framework describes the evolution of the system through three characteristic states, reflecting simultaneous changes in intensity, spatial structure, and stability of morphological processes (Figure 5).

In the initial stage (sediment-rich equilibrium), the system maintains a dynamic equilibrium state with abundant sediment supply. In this state, shoreline change rates are low (small LRR), erosion is relatively symmetrically distributed (low AI), and spatial variability is low (low CV), reflecting a stable system with morphological processes distributed relatively evenly.

When sediment supply begins to decline (transitional instability), the system shifts to an imbalanced state. This stage is characterized by a simultaneous increase in erosion intensity (|LRR| increases), asymmetry (AI increases), and spatial variability (CV increases). Erosion zones begin to form and concentrate spatially, reflecting the emergence of morphological “hotspots” and increasing system instability.

In the final stage (erosion-dominated structured regime), the system reaches a new morphological state after internal reorganization. Although erosion intensity remains high (large LRR) and asymmetry remains pronounced (high AI), spatial variability decreases (lower CV), indicating that erosion zones have been established and become more stable over time. This state reflects a system dominated by erosion but with a clearly structured spatial organization and lower variability.

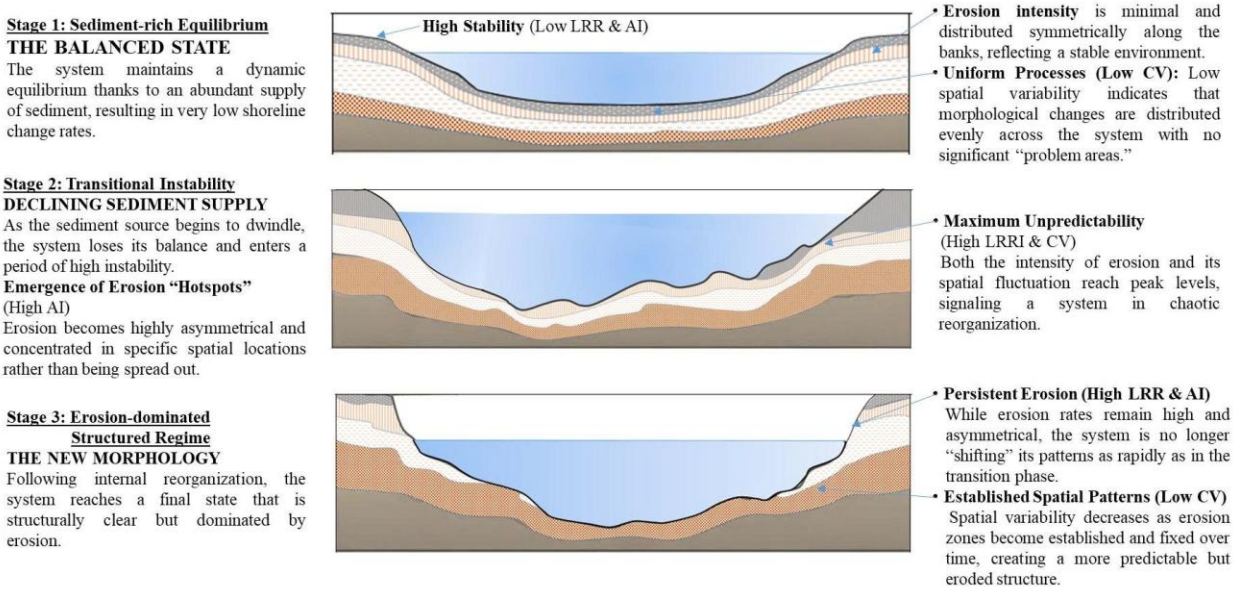

Figure 5. Conceptual framework of morpho-dynamic change under sediment starvation

This conceptual framework shows that sediment deficiency not only increases erosion intensity, but also triggers a process of spatial reorganization of the system, leading to a morpho-dynamic regime shift from a balanced state to an organized erosion-dominated state.

6. Conclusion

This study provides long term quantitative evidence of increasing bank erosion and spatial reorganization of the Vam Nao channel system under the impact of prolonged sediment deficiency, based on the integration of remote sensing data and spatial statistical analysis during the period 1988–2025. The results show a clear and consistent declining trend in sediment load at both Tan Chau and Vam Nao, reflecting a shift of the system from a sediment-rich state to a sediment-deficient state.

At the reach scale, shoreline analysis shows a strong increase in erosion during the period 1993–2011, especially in Area1 and Area4, with the appearance of continuously eroding right-bank segments and large negative LRR values. At the same time, the increase in AI indicates that erosion processes not only increased in intensity but also became asymmetric and skewed toward the right bank. In the period after 2012, although erosion intensity was maintained in some areas, the decrease in CV indicates that spatial variability has reduced, reflecting the relative stabilization of established erosion zones.

These results show that the morphological response of the system does not occur uniformly but exhibits clear spatial differentiation, including erosion-dominated, deposition-dominated, and transitional areas. This difference highlights the important role of local geometric and dynamic conditions in controlling morphological responses under sediment-deficient conditions.

Based on the obtained evidence, this study initially demonstrates that the Vam Nao channel system may have undergone a morphodynamic regime shift, expressed through three characteristic stages: (i) a relatively balanced state with abundant sediment supply, (ii) a highly dynamic phase with increased intensity and spatial heterogeneity of erosion, and (iii) a reorganized state in which erosion zones are established and more stable. This study contributes to the understanding of morphological dynamics in deltaic river systems under sediment deficiency, while emphasizing the importance of analyzing the spatial structure of erosion in addition to traditional aggregated indicators. The integrated approach combining long term remote sensing and morphological indexes can be applied to other river systems to identify early signals of morphodynamic regime shifts.

Authors' contributions

Nguyen Dam Quoc Huy: Conceptualization; Funding acquisition; Project administration; Methodology; Validation; Writing – original draft; Writing – review & editing. **Le Thi Thuy Van:** Visualization; Writing – original draft. **Tran Thi Kim**: Conceptualization; Methodology; Visualization; Writing – original draft.

Conflicts of interest

The authors have no competing interests to declare that are relevant to the content of this article.

Acknowledgment

This research is funded by Vietnam National University Ho Chi Minh City (VNU-HCM) under a project within the framework of the Program titled “Strengthening the capacity for education and basic scientific research integrated with strategic technologies at VNU-HCM, aiming to achieve advanced standards comparable to regional and global levels during the 2025–2030 period, with a vision toward 2045”

References

Allison M A, Nittrouer C A, Ogston A S, Mullarney J C and Nguyen T T 2017 Sedimentation and survival of the Mekong Delta: A case study of decreased sediment supply and accelerating rates of relative sea level rise *Oceanography* **30** 98-109 (https://www.jstor.org/stable/26201902)

Anthony E J, Brunier G, Besset M, Goichot M, Dussouillez P and Nguyen V L 2015 Linking rapid erosion of the Mekong River delta to human activities *Sci. Rep.* **5** 14745 (https://doi.org/10.1038/srep14745)

Blanckaert K, Duarte A and Schleiss A J 2010 Influence of shallowness, bank inclination and bank roughness on the variability of flow patterns and boundary shear stress due to secondary currents in straight open-channels *Adv. Water Resour.* **33** 1062-1074 (https://doi.org/10.1016/j.advwatres.2010.06.012)

Bozzano M, Varni F, De Martino M, Quarati A, Tambroni N and Federici B 2024 An integrated approach to riverbed morphodynamic modeling using remote sensing data *J. Mar. Sci. Eng.* **12** 2055 (https://doi.org/10.3390/jmse12112055)

Brousse G, Claude N, Cordier F, Loire R and Jodeau M 2024 2D morphodynamic modelling as a predictive tool for gravel replenishment: the Saint-Sauveur Dam case study *Int. J. River Basin Manage.* **22** 389-402 (https://doi.org/10.1080/15715124.2022.2153857)

Darby S E, Hackney C R, Leyland J, Kummu M, Lauri H, Parsons D R, Best J L, Nicholas A P and Aalto R 2016 Fluvial sediment supply to a mega-delta reduced by shifting tropical-cyclone activity *Nature* **539** 276-279 (https://doi.org/10.1038/nature19809)
Das P, Let S and Pal S 2013 Use of Asymmetry Indices and Stability Indices for Assessing Channel Dynamics: A Study on Kuya River, Eastern India *J. Eng. Comput. Appl. Sci.* **2** 24-31
Delong M D, Thorp J H and Anderson J R 2021 Ecological thresholds and regime shifts within hydrologically modified rivers: A 75+ year retrospective analysis *River Res. Appl.* **37** 54-63 (https://doi.org/10.1002/rra.3749)
Edmonds D A, Toby S C, Siverd C G, Twilley R, Bentley S J, Hagen S and Xu K 2023 Land loss due to human-altered sediment budget in the Mississippi River Delta *Nat. Sustainability* **6** 644-651 (https://doi.org/10.1038/s41893-023-01081-0)
Facun L P, Sta Maria M Y, Ducao R, Clemente J J, Carmelo E M, Maon A, Malaya A R, Cuison F and Siringan F 2025 QGIS Shoreline Change Analysis Tool (QSCAT): A fast, open-source shoreline change analysis plugin for QGIS *Environ. Model. Softw.* **184** 106263 (https://doi.org/10.1016/j.envsoft.2024.106263)
Feyisa G L, Meilby H, Fensholt R and Proud S 2014 Automated Water Extraction Index: A New Technique for Surface Water Mapping Using Landsat Imagery *Remote Sens. Environ.* **140** 23–35 (https://doi.org/10.1016/j.rse.2013.08.029)
Fisher A, Flood N and Danaher T 2016 Comparing Landsat water index methods for automated water classification in eastern Australia *Remote Sens. Environ.* **175** 167-182 (https://doi.org/10.1016/j.rse.2015.12.055)
Frascati A and Lanzoni S 2009 Morphodynamic regime and long-term evolution of meandering rivers *J. Geophys. Res.: Earth Surf.* **114** 1-12 (https://doi.org/10.1029/2008JF001101)
Ge H, Zhu L and Mao B 2025 Evolution of tidal reaches of the Yangtze River related to reduced non-uniform sediment after the impoundment of Three Gorges Reservoir *Catena* **260** 109462 (https://doi.org/10.1016/j.rsma.2024.103605)
Gierszewski P J, Habel M, Szmańda J and Luc M 2020 Evaluating effects of dam operation on flow regimes and riverbed adaptation to those changes *Sci. Total Environ.* **710** 136202 (https://doi.org/10.1016/j.scitotenv.2019.136202)
Gorelick N, Hancher M, Dixon M, Ilyushchenko S, Thau D and Moore R 2017 Google Earth Engine: Planetary-scale geospatial analysis for everyone *Remote Sens. Environ.* **202** 18-27 (https://doi.org/10.1016/j.rse.2017.06.031)
Hou X, Xie D, Feng L, Shen F and Nienhuis J H 2024 Sustained increase in suspended sediments near global river deltas over the past two decades *Nat. Commun.* **15** 3319 (https://doi.org/10.1029/2019JF005201)
Huy N D Q, Kim T T and An D T 2025 Hydrological Regime Variability between the Tien and Hau Rivers under the Impact of Anthropogenic Activities and Climate Change *J. Earth Environ. Sci. Res.* **7** 96-107 (https://doi.org/10.30564/jees.v7i5.8707)
Kendall M G 1975 *Rank Correlation Methods* (Charles Griffin London)
Knighton A 1981 Asymmetry of river channel cross-sections: Part I. Quantitative indices *Earth Surf. Processes Landforms* **6** 581-588 (https://doi.org/10.1002/esp.3290060607)
Kondolf G M, Rubin Z K and Minear J 2014 Dams on the Mekong: Cumulative sediment starvation *Water Resour. Res.* **50** 5158-5169 (https://doi.org/10.1002/2013WR014651Digital)
Kummu M, Lu X, Wang J-J and Varis O 2010 Basin-wide sediment trapping efficiency of emerging reservoirs along the Mekong *Geomorphology* **119** 181-197 (https://doi.org/10.1016/j.geomorph.2010.03.018)
Leopold L B, Wolman M G, Miller J P and Wohl E E 2020 *Fluvial Processes in Geomorphology: Second Edition* (Courier Dover Publications)
Li B, Yang H, Cai H, Ou S, Liu F, Zhao T, Lin K and Lin J 2025 Regime shift in river-tide dynamics of longitudinal and transverse channels over the Pearl River Delta, China *J. Hydrol.* **662** 133883 (https://doi.org/10.1016/j.jhydrol.2025.133883)
Ma L, Ding D, Wang G, Huang Y, Lv Y and Li G 2025 Analysis of the evolution of the current estuarine geomorphology of the Yellow River under 20 years of water and sediment regulation *J. Hydrol.* **646** 132344 (https://doi.org/10.1016/j.jhydrol.2024.132344)
Mcfeeters S 1996 The Use of Normalized Difference Water Index (NDWI) in the Delineation of Open Water Features *Int. J. Remote Sens.* **17** 1425-1432 (https://doi.org/10.1080/01431169608948714)
Murphy J, Schafer L A and Mize S 2025 Tracking persistent declines in suspended sediment in the Lower Mississippi and Atchafalaya Rivers, 1992–2021: Harnessing WRTDSplus to characterize longitudinally varying trends and explore connections to streamflow *J. Hydrol.* **662** 133885 (https://doi.org/10.1016/j.jhydrol.2025.133885)
Nga T N Q, Kim T T, Nghia H H, Hoai H C and Bay N T 2022 *IOP Conf. Ser.: Earth Environ. Sci* **1091** 012016 (https://doi.org/10.1088/1755-1315/1091/1/012016)
Paola C and Voller V R 2005 A generalized Exner equation for sediment mass balance *J. Geophys. Res.: Earth Surf.* **110** (https://doi.org/10.1029/2004JF000274Digital)
Pettitt A N 1979 A non-parametric approach to the change-point problem *J. R. Stat. Soc., C: Appl. Stat.* **28** 126-135 (https://doi.org/10.2307/2346729)
Phillips C B, Masteller C C, Slater L J, Dunne K B, Francalanci S, Lanzoni S, Merritts D J, Lajeunesse E, Jerolmack D J J N R E and Environment 2022 Threshold constraints on the size, shape and stability of alluvial rivers *Nat. Rev. Earth Environ.* **3** 406-419 (https://doi.org/10.1038/s43017-022-00282-z)
Şen Z 2012 Innovative Trend Analysis Methodology *J. Hydrol. Eng.* **17** 1042-1046 (https://doi.org/10.1061/(ASCE)HE.1943-5584.0000556)

Tanwari K, Terefenko P, Shi X, Śledziowski J and Giza A 2025 Coastal zones vulnerability evaluation in the southern Baltic Sea: Shoreline dynamics and land use/land cover changes over five decades *Sci. Total Environ.* **976** 179345 (https://doi.org/10.1016/j.scitotenv.2025.179345)
Van Binh D, Kantoush S and Sumi T 2020 Changes to long-term discharge and sediment loads in the Vietnamese Mekong Delta caused by upstream dams *Geomorphology* **353** 107011 (https://doi.org/10.1016/j.geomorph.2019.107011)
Van Manh N, Dung N V, Hung N N, Kummu M, Merz B and Apel H 2015 Future sediment dynamics in the Mekong Delta floodplains: Impacts of hydropower development, climate change and sea level rise *Glob. Planet. Change* **127** 22-33 (https://doi.org/10.1016/j.gloplacha.2015.01.001)
Wang S 2025 Differential changes in water and sediment transport under the influence of large-scale reservoirs connected end to end in the upper Yangtze River *Hydrology* **12** 292 (https://doi.org/10.3390/hydrology12110292)
Wang Z, Van Maren D, Ding P, Yang S, Van Prooijen B, De Vet P, Winterwerp J, De Vriend H, Stive M and He Q 2015 Human impacts on morphodynamic thresholds in estuarine systems *Cont. Shelf Res.* **111** 174-183 (https://doi.org/10.1016/j.csr.2015.08.009)
Wen Y, Li P, Li M, Ma C, Gao P, Mu X and Zhao G 2025 Changes in River Cross-section Morphology and Response to Streamflow and Sediment Processes in Middle Reaches of Yellow River, China *Chin. Geogr. Sci.* **35** 161-174 (https://doi.org/10.1007/s11769-025-1488-3)
Wu G, Wang K, Liang B, Wu X, Wang H, Li H and Shi B 2023 Modeling the morphological responses of the Yellow River Delta to the water-sediment regulation scheme: The role of impulsive river floods and density-driven flows *Water Resour. Res.* **59** e2022WR033003 (https://doi.org/10.1029/2022WR033003Digital)
Xu H 2006 Modification of normalised difference water index (NDWI) to enhance open water features in remotely sensed imagery *Int. J. Remote Sens.* **27** 3025-3033 (10.1080/01431160600589179)
Xu N 2018 Detecting Coastline Change with All Available Landsat Data over 1986–2015: A Case Study for the State of Texas, USA *Atmosphere* **9** 107 (https://doi.org/10.3390/atmos9030107)
Zhu Q, Xing F, Wang Y P, Syvitski J, Overeem I, Guo J, Li Y, Tang J, Yu Q and Gao J 2024 Hidden delta degradation due to fluvial sediment decline and intensified marine storms *Sci. Adv.* **10** eadk1698 (https://doi.org/10.1126/sciadv.adk1698)